B-HADRON LIFETIMES

W. B. ATWOOD AND J. A. JAROS

Stanford Linear Accelerator Center
Stanford University, Stanford, CA 94309

ABSTRACT

The theory and practice of measuring B-hadron lifetimes, and extracting the Cabibbo-Kobayshi-Maskawa (CKM) matrix element V_{cb} are reviewed. Experiments from CESR, DORIS, PEP, PETRA, LEP, and Fermilab are included to form an up-to-date compilation of the experimental results.The generic lifetime measurement techniques, the just-now-emerging meson-specific vertexing methods, as well as indirect methods for measuring lifetime ratios, are discussed

1. Introduction

In 1983, the MAC [1] and MARK II [2] Collaborations at PEP discovered that the impact parameters of prompt leptons produced in high energy e^+e^- annihilations were on average discernibly positive, and they inferred that the B-hadron lifetime was about 1 ps. The result was unexpected. A recent paper [3] had predicted that the B lifetime was less than 0.12 ps, although a more conservative analysis [4] could accommodate picosecond lifetimes. The only phenomenological guide to the strength of the intergenerational mixing responsible for the decay was (and is) the magnitude of the Cabibbo angle. If mixing between the second and third generations had the same strength as that between the first and second, the B lifetime would be about 0.1 ps. Experimentally, the failure to find long-lived, massive particles produced in hadronic [5] and e^+e^- [6] interactions implied $\tau_B < 5 \times 10^{-8}$ s and $\tau_B < 2 \times 10^{-9}$ s, respectively. The year before the 1983 discovery, the JADE [7] experiment at PETRA introduced the essential elements of the lepton impact parameter method in setting a much improved upper limit on the lifetime, $\tau_B < 1.4$ ps. The year after the discovery saw its confirmation by the DELCO experiment at PEP and the TASSO and JADE experiments at PETRA.

The implications of the new result were felt almost immediately. Studies of the endpoint of the B semileptonic decay spectrum at Cornell [8] had shown that the b quark couples predominantly to the charmed quark. In terms of the CKM matrix elements, the B lifetime therefore depends essentially on the single unknown parameter $|V_{bc}|$. The early lifetime measurements thus provided the first measure of the magnitude of V_{bc}. Along with measurements of the ratio $|V_{bu}| / |V_{bc}|$ from Cornell, and the unitarity constraints on the CKM matrix, the determination of $|V_{bc}|$ led to the first complete picture of the magnitudes of all the CKM elements [9]. It was rapidly appreciated that a long B lifetime had interesting

To be published in "B Decays," edited by S. Stone

consequences, including measurable $B\bar{B}$ mixing [10] and a lower limit on the top quark mass [11]. It had experimental consequences, too: it is possible to identify high energy b-quark jets by observing the decay vertices of the B and C hadrons.

Most of the results described below come from studies of e^+e^- annihilations performed at the e^+e^- storage ring facilities. The e^+e^- environment has had a near monopoly on the field because B hadrons are produced in sufficient quantity for lifetime studies, and more importantly, because the B hadron sample is identified with comparative ease and cleanliness. B hadrons produced in e^+e^- annihilations constitute a significant fraction of all hadronic events. The B mesons produced nearly at rest in $\Upsilon(4S)$ decays at CESR and DORIS II account for more than 25% of the total hadronic cross section. At PEP and PETRA, B hadron jets account for 9% of the hadronic cross section, and at LEP, B hadrons are produced in 22% of the hadronic decays of the Z^0. Hadronic production of B hadrons occurs with much higher absolute cross section, but comprises a very much smaller fraction of the total interaction rate. To date, only emulsion experiments have succeeded in isolating a clean B hadron signal for lifetime measurements in this environment. But changes can be expected.

In the following, we review the physics of B-hadron lifetimes, discuss in some detail impact parameter measurements of τ_B, and review other measurements of average B lifetimes. We then turn to measurements of particular B-meson lifetimes and the ratio of the charged-to-neutral lifetimes. We conclude with an outlook and summary. We have attempted to include all experimental results, circa summer 1991. If we have not succeeded, be assured it was an error of omission, not editorial malice.

2.   Physics of B Lifetimes

In this section we will explore the underlying physics of B-hadron lifetimes. The total width for the decay of b quarks may be broken into two terms, one for semileptonic decays and one for hadronic decays:

$$\Gamma_{\text{TOT}} = \Gamma_{\text{sl}} + \Gamma_{\text{had}} . \tag{1}$$

The lifetime is simply the reciprocal of the total width and can be related to the width of a specific channel in terms of the branching ratio for that channel. Specifically [12],

$$\tau_b = \frac{1}{\Gamma_{\text{TOT}}(b)} = \frac{B_{r_{\text{sl}}}}{\Gamma_{\text{sl}}} . \tag{2}$$

The selection of semileptonic decays is not accidental. As was pointed out in Chap. 5 of this volume, the semileptonic channels have the fewest uncertainties in the extraction of Standard Model parameters. Furthermore, the semileptonic branching ratio (Br_{sl}) is the best measured, thereby introducing the least uncertainty, as well.
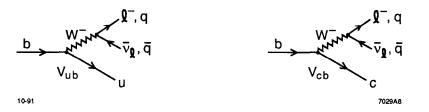
Fig. 1. Contributions to b quark decay. The amplitude for each diagram is proportional to the CKM matrix terms V_{ub} and V_{cb} respectively. The $q\bar{q}$ pair produced can be any of the quark combinations present in the CKM matrix.

The lifetime equation (2) has been written in terms of the b quark, but of course must be related to b hadrons. The simplest model used to describe this situation is the "spectator model" and is shown diagrammatically in Fig. 1. In the Standard Model, b quarks decay to either c or u quarks by coupling to the electroweak charged current, the W. The off-shell W subsequently decays to either a leptonic (e.g., $\bar{\nu}_e e$) or a quark doublet (e.g., $\bar{u}d$). In the spectator model, the other quarks are assumed to have a negligible effect on the b quark decay and are merely "spectators." It is widely accepted that the spectator model well describes semileptonic decay. Within this framework, all mesons and baryons containing a b quark will have approximately the same lifetime. Alternatives and embellishments will be examined later.

The width is calculable from the known properties of the electroweak current and the couplings of one quark generation to another, usually described by the Cabibbo-Kobayshi-Maskawa (CKM) mixing matrix V_{qQ} (Rosner discusses the Cabibbo-Kobayshi-Maskawa Matrix in Chap. 9 of this volume). In order to simplify the discussion, we restrict ourselves to semileptonic decays. The matrix element for b quarks decaying to lighter quarks q may be expressed as the product of a leptonic and hadronic current:

$$M_{\text{sl}} = -\frac{G_F}{\sqrt{2}} V_{qb} \left[\bar{q}\, \gamma^\mu(1-\gamma_5)\, b \right] \left[\bar{\ell}\gamma_\mu(1-\gamma_5)\, \nu_\ell \right]. \tag{3}$$

This matrix element is the same as that in muon decay with the hadronic current replaced by an analogous muon term. G_F is the Fermi coupling constant. After squaring M_{sl} and integrating over phase space, the well known decay rate is given by

$$\Gamma_{\text{sl}}(b \to q) = \frac{G_F^2\, m_b^5}{192\pi^3}\, |V_{qb}|^2\, F(\epsilon), \tag{4}$$

where $F(\epsilon)$, the phase space factor, is given by

$$F(\epsilon) = 1 - 8\epsilon^2 + \epsilon^6 - \epsilon^8 - 24\,\epsilon^4\, \ell n\,\epsilon \tag{5}$$

and $\epsilon \equiv m_q/m_b$. (For a more complete discussion of Eqs. 4 and 5, see Rosner in Chap. 9 of this volume.)

In the Standard Model, in as much as b quarks only decay into u and c quarks, τ_b measures a combination of $|V_{ub}|^2$ and $|V_{cb}|^2$:

$$\tau_b = \frac{B_{r_{sl}}}{\Gamma_{sl}} = \frac{B_{r_{sl}}}{\left\{ \frac{G_F^2 \, m_b^5}{192\pi^3} \, [F(\epsilon_u) \, |V_{ub}|^2 + F(\epsilon_c) \, |V_{cb}|^2] \right\}} \, . \tag{6}$$

We also know from fits to prompt lepton spectra [13] at the Υ_{4s} that $|V_{ub}|^2 \ll |V_{cb}|^2$ (indeed $|V_{ub}|^2 / |V_{cb}|^2 \sim 10^{-2}$). Thus τ_b is mainly a measurement of $|V_{cb}|$.

From Eq. 6, it is apparent that the extraction of $|V_{cb}|$ from B-hadron lifetimes relies on estimates of the masses of the various quarks involved. For m_b, an *effective* b quark mass is used. A popular way to estimate this effective mass is in the context of the ACM model [14]. Kinematic effects due to Fermi motion are included in this model and the momentum wave function for the B hadron is obtained by fitting the experimental spectrum of prompt leptons from B decays. Effects of gluon radiation have also been included in the ACM model. Both the CLEO and ARGUS Collaborations have made such fits for B mesons produced at the Υ_{4s} with the results [15]:

$$\langle m_b \rangle = \begin{cases} 4.95 \pm .04 \text{ GeV}/\text{c}^2 & \text{(CLEO)} \\ 4.95 \pm .07 \text{ GeV}/\text{c}^2 & \text{(ARGUS)} \, . \end{cases} \tag{7}$$

Another approach to reducing the uncertainty introduced by m_b is to observe that when the mass difference $m_b - m_c$ is constrained, the combination $m_b^5 \, F(\epsilon_c)$ is well determined. A *measured* value for $m_b - m_c$ also comes from the fits to prompt lepton spectra and is quite stable. The resulting uncertainty in the extraction of $|V_{cb}|^2$ is much the same as when tight mass limits are used on m_b alone, and this method may be less model dependent [16].

QCD Radiation Effects

The quarks involved in the decay of b hadrons may radiate gluons which in turn materialize into more hadrons. The inclusion of this radiation in the expression for Γ_{sl} (Eq. 6) results in a multiplicative factor of $[1 - (2\alpha_s/3\pi) \, g \, (\epsilon)]$ and is similar to the correction in muon decay accounting for QED radiation, substituting α_s for α. The function $g(\epsilon)$ (where again $\epsilon \equiv m_q/m_b$) may be approximated numerically by [17]

$$g(\epsilon) = \left(\pi^2 - \frac{31}{4} \right) (1 - \epsilon)^2 + \frac{3}{2} \tag{8}$$

and for values of $\epsilon_{c(u)} = 1.65/4.95(.20/4.95)$ evaluates to 2.44 (3.45). Using a value of $\alpha_s = .20$ [18] results in a QCD radiation correction of -10.4% and -14.6% for the $b \rightarrow c$ and $b \rightarrow u$ transitions.

The results so far with $m_b = 4.95 \text{ GeV}/\text{c}^2$, $\text{m}_c = 1.65 \text{GeV}/\text{c}^2$, and $m_u = .2 \text{ GeV}/\text{c}^2$ can be summarized by

$$\Gamma_{sl} = 2.67 \times 10^{-11} \left[|V_{cb}|^2 + 2.15 \, |V_{ub}|^2 \right] \text{ (GeV)} \, . \tag{9}$$

4

Form Factors and Wave Functions

Effects other than the kinematic effects included in the ACM model require detailed models of the wave functions of the specific hadrons in which the quarks reside. The quarks fields in Eq. 3 for the matrix element need to be replaced by hadrons in the initial and final state. Two practical problems arise. First, there exist only approximate models for hadrons based on various parameterizations of the effective QCD potential. Second, in principle, a calculation must be made for each decay channel that is included in the measurement, potentially a formidable task even for inclusive semileptonic decays. There are several attempts to do this, but we'll restrict ourselves to two.

The approach of Wirbel, Stech, and Bauer (WSB model [19]) is to start with a general expression for form factors arising in hadronic currents. Using a simple ansatz for these form factors, and evaluating constants appearing in their results in terms of meson wave functions from a relativistic harmonic oscillator model, they find (with $\alpha_s = .20$)

$$\Gamma_{sl} = 2.22 \times 10^{-11} \left[|V_{cb}|^2 + 1.65 |V_{ub}|^2\right] \quad (\text{GeV}) \quad . \tag{10}$$

This result is about 20% lower than obtained in the ACM model, which may be due to the limited number of final states summed over. Specifically the WSB model includes B meson decays to D, D^*, ρ, and π mesons, as would be appropriate for calculating the spectrum of the most energetic prompt leptons.

The more recent work of Isgur, Scora, Grinstein, and Wise (ISGW model [20]) pursues a similar calculation. They choose to express the square of the hadronic current as sums and differences of the initial and final meson four-momenta times form factors. The form factors are then calculated using meson wave functions derived from a Coulomb plus linear QCD potential. All meson final states are summed over for $1S$, $2S$, and $1P$ wave functions, and the final result is

$$\Gamma_{sl} = 2.70 \times 10^{-11} |V_{cb}|^2 \quad (\text{GeV}) \quad , \tag{11}$$

which is remarkably close to the ACM results.

The main emphasis of both of the above calculations is to compute the spectrum of prompt electrons arising in these decays. Of particular interest is the shape and size of the electron spectrum beyond the kinematic endpoint allowed in $b \to c$ transitions. An accurate model for this part of the prompt electron spectrum would allow the extraction of V_{ub}. The calculation of the overall semileptonic decay rate is more or less a by-product of this effort. What is germane to this discussion is that the rate calculations using specific wave function models are in accord with the quark-level dynamics of the ACM model

Expectations for Lifetimes of Specific B Mesons

Lifetime differences may be used to test specific models and mechanisms involved in B-hadron decays [21]. It is widely believed that as the quark mass increases, the lifetimes of different types of hadrons carrying the quark will approach one another. As Bigi points out in Chap. 3, there is no rigorous proof of this conjecture, but it does seem to match experimental observation. Also among B hadrons,

the expectation is for an ordering of lifetimes, $\tau(\Lambda_b) < \tau(B^0) < \tau(B^{\pm})$, analogous to what is found experimentally in charm decays.

3. Impact Parameter Measurements

Although B-hadron lifetimes are too short to be measured directly with timing techniques, they can in principle be measured by simultaneously determining the B decay lengths, $\ell = \gamma\beta \, c \, \tau_B$, and the B momenta, from which the factor $\gamma\beta$ can be derived. In practice, this technique has been of little use because it is difficult to associate exactly which of the particles produced in a hadronic jet containing a B hadron are its direct decay products, which are fragmentation debris, and which are associated with the decay of the daughter charmed hadron. Consequently neither the B decay length, nor its momentum is precisely determined. A complementary approach has proved effective. By virtue of the finite flight path of the B, a lepton originating in its decay will appear to "miss" the primary interaction point where the B was created. The miss distance, or impact parameter, of this lepton is a measure of the lifetime, and its value, averaged over all decay lengths and decay kinematics, is proportional to the particle lifetime. The lepton is an especially suitable decay product for study since it is tied to the primary B decay and its decay distributions are well known. The first B lifetime measurements exploited these features to make credible measurements, and the best measurements of the average B lifetime done to date still use this technique. In this section, we will discuss this method in some detail, and summarize the current state of the measurements. We will additionally discuss B-hadron lifetime measurements derived from measurements of the impact parameters of all charged particles originating in hadronic jets that contain B hadrons.

Event Selection

Ideally, as mentioned above, one measures the impact parameter of a lepton originating in the decay of a B hadron. In practice, this is accomplished by identifying an electron or muon in a hadronic event that has high (typically ≥ 1 GeV/c) momentum transverse (p_T) to the jet direction in the event. Thrust, sphericity, and more recently cluster algorithms [22], have been used to estimate the jet direction. The prompt lepton signal in e^+e^- annihilations is due primarily to the semileptonic decays of charm and bottom quarks. The maximum transverse momentum that a lepton from the decay of a quark of mass m_q may have is $\sim m_q/2$. The bottom quark, with roughly three times the charm quark mass, thus accounts for most of the lepton signal beyond $p_T \sim m_c/2$. Hard gluon bremsstrahlung in $c\bar{c}$ events can perturb the estimate of the jet direction enough to contaminate the high-p_T region. Analyses [23] of the inclusive lepton spectra in e^+e^- annihilations have led to a quantitative understanding of the high-p_T lepton signal, and to the fragmentation properties of heavy quarks, both essential ingredients for determinations of the B lifetime. Figure 2 shows a recent measurement [23] of the transverse momentum spectrum of leptons observed in hadronic decays of the Z^0. It is apparent that most of the high transverse momentum component is due to direct leptonic decays ($b \rightarrow \ell \bar{\nu} c$) and cascade decays ($b \rightarrow c \rightarrow \ell \bar{\nu} x$) from B hadrons. Table 1 itemizes several

Table I. Comparison of lepton impact parameter measurements.

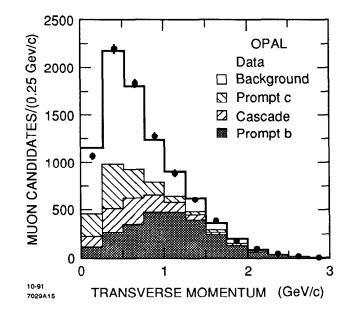| Experiment	Lepton Identification e	Lepton Identification μ	B-Region Selection Cuts (GeV/c)	Fraction of Lepton Candidates from B Decay	Number of Leptons	$\langle\sigma_\delta\rangle$ [μm]
MAC	Pb/Gas Calorimeter	Magnetized Fe Absorber Hadron Calorimeter	$p > 2$ $p_T > 1.5$	0.70	398	600
MARK II	Pb/Liquid Argon	Fe Absorber	$p > 2$ $p_T > 1$	0.64	617	161
DELCO	Pb/Scintillator Calorimeter + Čerenkov	——	$p_T > 1$	0.79	113 e	400
HRS	Pb/Scintillator Calorimeter	——	$p > 2$ $p_T > 1.1$	0.53	301 e	400
JADE	Pb Glass Calorimeter + dE/dx	Fe Absorber	$p > 1.5$ $p_T > 0.9$	0.71 e 0.88 μ	(1986) 74 μ; 25 e (1989) 81 μ; 65 e	570 350
ALEPH	Pb Glass Calorimeter + dE/dx	Hadron Calorimeter + Absorber	$p > 5$ $p_T > 2$	0.73	1215 e 1758 μ	200
DELPHI	——	Magnetized Fe Absorber	$p > 3$ $p_T > 1$	0.64	839 μ	84
L3	BGO Calorimeter	Hadron Calorimeter + Magnetized Fe Absorber	$p > 4$ $p_T > \begin{cases} 1.5\ \mu \\ 1.0\ e \end{cases}$	0.89 e 0.87 μ	673 e 713 μ	216
OPAL	Pb Glass Calorimeter + dE/dx	Hadron Calorimeter + Absorber	$p > 4$ $p_T > 1.5$	0.86 e 0.81 μ	667 e 783 μ	120

7

Fig. 2. Transverse momentum spectrum of muons in hadronic Z^0 decays.

important features of the lepton samples used by experiments to measure lepton impact parameters. Of the experiments at low energy [24], DELCO has exceptional sample purity, accomplished by combining Čerenkov information with the other electron identification tools. The LEP experiments [25] boast the largest and cleanest lepton samples to date. Their advantage stems from the high cross section for $b\bar{b}$ production at the Z^0, the improved signal (b) to background (c) rates at the Z^0 in comparison to the low energy continuum, and the ease in identifying very high momentum leptons.

Other techniques have been used to enrich the fraction of $b\bar{b}$ events over the nominal $1/11$ expected in the continuum. Both the JADE and TASSO experiments have used the sphericity product $S_1 \times S_2$ to discriminate between $b\bar{b}$ and light-quark events. After excluding obvious 3-jet candidates, the experimenters determine the sphericity axis and divide the tracks two sphericity hemispheres. They then compute the sphericity of each hemisphere in a frame boosted to B-like velocity in the jet direction. B jets on average have higher sphericities than lighter quark jets, so B events have higher sphericity products. Figure 3 shows the distribution of $S_1 \times S_2$ for b quarks and the lighter quarks. The calculation of these distributions depends on detailed Monte Carlo simulations, and is subject to comparatively large systematic errors.

The MARK II Collaboration at SLC has recently used a lifetime tag [26] to identify $Z^0 \to b\bar{b}$ events. The tag is 50% efficient and the sample purity is 85%, making this potentially the most powerful way to tag B hadron events in e^+e^- annihilations.

Impact Parameter Definition

All experiments to date have measured the impact parameters of tracks projected into the plane (x, y) perpendicular to the beam axis. It is in this plane that the
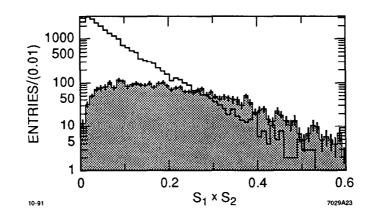
Fig. 3. Sphericity product distribution for b-quark production (shaded area) and $udsc$-quark production in e^+e^- annihilations at $\langle\sqrt{s}\rangle = 36.3$ GeV. The distributions have been calculated by the JADE (90) experiment [24].

luminous region is small, and in this plane that charged particle trajectories have been measured with high precision. Figure 4 illustrates the quantities used in defining the impact parameter. The luminous region in an e^+e^- collider typically has a rms height of tens of microns, a rms width of several hundred microns, and a well-defined and stable beam center. A B hadron is produced in the vicinity of the beam center at the primary interaction point, and travels on average about .3 $\gamma\beta$ [mm] before decaying at a secondary vertex. A charmed
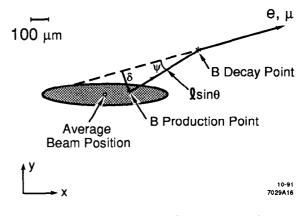

Fig. 4. Definition of the projected impact parameter δ.

meson produced in the B decay travels further, decaying at a tertiary vertex. The lepton produced at the secondary vertex has an impact parameter $\delta = \gamma\beta c\tau_B |\sin\theta| \sin\psi$, where τ_B is the proper lifetime of the B hadron, θ is the angle between the B hadron and the beams, and ψ is the angle between the lepton trajectory and the B-hadron direction, projected onto the x-y plane. In the limit that the B is highly relativistic, the average impact parameter becomes independent of the B momentum, since the increase in the average decay length ($\gamma\beta c\tau_B$) is compensated by the decrease in the average decay angle ($\sin\psi \propto \gamma^{-1}$). As a rule of thumb, $\langle\delta\rangle \sim c\tau$. The dependence of the average lepton impact parameter on B momentum [27], including the acceptance effects imposed by momentum thresholds for lepton identification, is shown in Fig. 5. As the figure suggests, the average lepton impact parameter is insensitive to the momentum distribution of B's at Z^0 energies, where $\langle p_B\rangle \approx 30$ GeV/c.
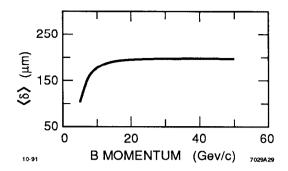
9

Fig. 5. The average lepton impact parameter versus B momentum. This calculation includes the effects of lepton selection and event acceptance cuts. The average B momentum at PEP/PETRA is about 10 GeV/c, and at LEP about 30 GeV.

Measuring the Impact Parameter

Impact parameter measurements require the determination of the primary interaction point, the lepton trajectory, and the B hadron direction. The average beam position is an unbiased estimator of the primary interaction point, and is easily measured by finding the average intercepts of nearly horizontal and nearly vertical tracks. This procedure finds the beam center with ~ 25 μm accuracy over the course of a several-hour fill, during which time the position is usually stable. The measurement also provides an estimate of the horizontal and vertical beam sizes, which, as discussed below, are important components of the impact parameter resolution. Some experiments have monitored beam stability over shorter periods with beam position monitor information, and discarded data associated with errant beam positions. Since the horizontal beam size at e^+e^- storage rings is comparable to or larger than the average impact parameter expected in B-hadron decays, the MARK II (89) and DELPHI (91) experiments have improved on the estimation of the primary interaction point by using information from other charged tracks in the event. The MARK II experiment, for example, was able to reduce the average impact parameter error from 291 to 161 μm.

The lepton trajectory is determined by fitting the data from charged particle tracking detectors. Most experiments have augmented the central tracking chambers with vertex detectors, high resolution tracking devices positioned as close as possible to the interaction point. In the e^+e^- collider environment, the interaction takes place within very high vacuum, in a beam chamber passing axially through the detector. The tracks measured by the devices outside this chamber are extrapolated typically 5 or 10 cm to the vicinity of the primary interaction. Multiple Coulomb scattering in the beam pipe and surrounding tracking detectors is a significant component of the extrapolated track resolution for tracks with $p < 3$ GeV/c, and is minimized by reducing the beam chamber radius, using low Z materials for the chamber, and minimizing its thickness. Most measurements to date have exploited precision drift chambers, which have a point measuring accuracy of about 100 μm. DELPHI (91) has reported results using silicon microstrip detectors, with a point resolution ~ 10 μ. As can be seen from Table 1, most experiments have had resolutions at best slightly larger than the average lepton impact parameter ($\langle \delta_\ell \rangle \sim 150$ μm), and accordingly suffer some loss of statistical sensitivity. Very high resolution devices, with $\sigma_\delta \ll \langle \delta_\ell \rangle$, promise to reduce the sensitivity of the fits to details of the detector response, a significant systematic error. For purposes of precision tracking, each of the experiments imposes tight restrictions on the quality of tracks accepted for analysis. The tracking resolution can be measured in $e^+e^- \rightarrow e^+e^-$ or $e^+e^- \rightarrow \mu^+\mu^-$ events by studying

the distance between the two final state tracks after extrapolation to the vicinity of the primary interaction point, and the impact parameter resolution by studying the impact parameter distribution of hadron tracks in unenriched hadronic events.

The impact parameter is ideally a positive definite quantity, reflecting the fact that the decay length is positive definite. Experimentally, it has been useful to *sign* the impact parameter by effectively measuring the sign of the decay length. The B hadron is assumed to originate at the production point, travel along the jet axis as estimated by the thrust (or sphericity, or cluster) direction, and decay to a lepton whose trajectory makes an acute angle with respect to the B-hadron trajectory. The intersection of this B hadron trajectory with that of the decay lepton gives rise to a positive or negative decay length, and the impact parameter is signed accordingly. The measured impact parameter can be negative because of errors made in assigning the production point or measuring the lepton trajectory, because the B-hadron direction is estimated incorrectly, or because leptons from the B decay appear or are backwards in projection. In the limit of perfect impact parameter resolution, where the production point and lepton trajectory are perfectly known, uncertainties in the estimated B direction still give rise to negative impact parameters. Figure 6(a) shows the results of a Monte Carlo calculation of the resultant lepton impact parameter distribution, and shows a slight negative tail. The effect is relatively minor in the case of B decays because the error in estimating the B-hadron direction [28], $\langle \Delta\phi \rangle \approx .1$, is significantly smaller than the average projected decay angle, $\langle \psi \rangle \approx .3$. These same effects are much more significant for charm decays because the average decay angle is more nearly comparable to the error in estimating the c hadron direction. The mean lepton impact parameter from charm decays is consequently much smaller than that from B decays. The mean impact parameters of muons from π and K decays are, for the same reason, very small, although the individual impact parameters can be significant.
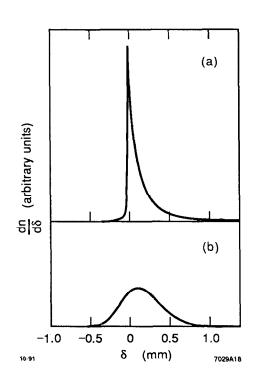

Fig. 6. Lepton impact parameter distribution for leptons from primary B decays before (a) and after (b) resolution smearing. The effect of jet direction uncertainties has been included in (a), contributing a small negative tail.

The effect of including the finite impact parameter resolution is illustrated in Fig. 6(b) for the case $\sigma_\delta \sim 2 \langle \delta_\ell \rangle$, and can be seen to be the convolution of the near Gaussian resolution with the primordial impact parameter distribution. The mean

11

of the primordial distribution is of course left intact. The resultant lepton impact parameter distribution is a slightly skew Gaussian with a positive mean, and a trace of exponential tail at high impact parameter.

Impact Parameter Distributions

All the recent analyses of lepton impact parameter measurements have followed the technique introduced and developed by the MARK II group [28]. In this analysis, the lepton impact parameter distribution is written as the sum of the impact parameter distributions from five sources: primary B-hadron leptons, cascade B hadron leptons (i.e., those from semileptonic decays of charmed particles produced in B decays), primary C hadron leptons, leptons arising from decays of pions and kaons, and hadrons which have been misidentified as leptons. The impact parameter distribution is written:

$$ P(\delta) \;=\; f_b\, P_b(\delta, \tau_b) \;+\; f_{bc}\, P_{bc}(\delta, \tau_b, \tau_c) + f_c\, P_c(\delta, \tau_c) + f_{dk}\, P_{dk}(\delta) + f_{\mathrm{mis}} P_{\mathrm{mis}}(\delta) \; , \quad (12) $$

where the individual distributions are each normalized to 1, and the terms are weighted by factors f_i, which are the fractions of the overall sample due to process i. The factors are known from inclusive lepton analyses. The sample purities $(f_b + f_{bc})$, which have been summarized in Table 1, are seen to range from about 60% to above 85%. Additional backgrounds from photon conversions and Dalitz decays have generally proved inconsequential. Experiments working in the e^+e^- continuum have exercised care to exclude contamination from tau pair production and, more significantly, from deep inelastic 2-photon interactions.

The distribution of projected impact parameters can be expressed analytically [29], in the limit of very high energies, in terms of the scaled impact parameter $y \equiv \delta/c\tau$ as

$$ P(y) = \int\limits_{0}^{\infty} \frac{2yz^2}{(z^2 + y^2)^2} \; e^{-z} \, dz \quad . \tag{13} $$

At nonasymptotic energies, and in order to incorporate the effects of experimental acceptance cuts, it is necessary to calculate this distribution with Monte Carlo techniques. These calculations include accurate modeling of B production and decay, event and acceptance cuts, and jet direction uncertainties. Resolution smearing is explicitly postponed to a later stage. The result of such a calculation for $P_b(\delta, \tau_b)$ is shown in Fig. 7. Both the positive and negative parts of the distribution can be parameterized as the sum of two exponentials. It is then easy to calculate the distribution at one particular B lifetime, and simply scale the distribution to other values of the lifetime. In the MARK II analysis, for example, the mean of the distribution is 143 μm for $\tau_B = 1$ ps. The functions $P_{bc}(\tau_b, \ \tau_c)$ and $P_c(\tau_c, \ \delta)$ are determined similarly, using the known charm lifetimes. Although the function $P_{bc}(\tau_b, \tau_c, \ \delta)$ does not strictly scale with the B lifetime (clearly $\langle \delta \rangle_{bc}$ is not zero when τ_b=0), for B lifetimes near 1 ps, it is seen to scale approximately. It should also be noted that
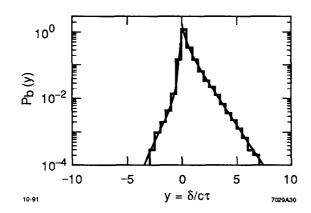
Fig. 7. The lepton impact parameter distribution from primary B decays used in fitting the observed impact parameter distribution. The distribution can be fit with the sum of two exponentials in each of the $y > 0$ and $y < 0$ regions. The resultant fit is shown.

$P_{bc}(\delta) \approx P_b(\delta)$. The mean impact parameters of the cascade and charm lepton distributions are $\langle \delta_{bc} \rangle = 167$ μm and $\langle \delta_c \rangle = 40$ μm. The distribution $P_{\mathrm{mis}}(\delta)$ is determined by measuring the impact parameter of hadrons which satisfy the same kinematic selection criteria as the lepton sample. The decay distribution $P_{dk}(\delta)$ is determined by Monte Carlo techniques.

Resolution effects are included by convoluting the distributions with the resolution function, $R(\delta, \sigma_\delta)$.

$$P_b'(\delta,\ \sigma_\delta,\ \tau_b) \ = \ \int \, d\epsilon \ P_b(\epsilon,\ \tau_b) \, R(\delta - \epsilon,\ \sigma_b) \quad . \tag{14}$$

If P_b is parameterized as a sum of exponentials, and the resolution function as a sum of Gaussians, then the integral can be done analytically. The impact parameter resolution σ_δ has contributions from the resolution of the extrapolated trajectory σ_{tr} (including multiple Coulomb scattering) and from uncertainties in the position of the primary interaction point, σ_{IP}.

$$\sigma_\delta^2 \ = \ \sigma_{tr}^2 + \sigma_{\mathrm{IP}}^2 \quad . \tag{15}$$

For the case where the average beam position approximates the interaction point,

$$\sigma_{\mathrm{IP}}^2 \ = \ \sigma_x^2 \sin^2 \phi + \sigma_y^2 \cos^2 \phi \quad , \tag{16}$$

where the beam size is $\sigma_x \times \sigma_y$, and ϕ is the azimuthal angle of the lepton trajectory. It has become commonplace to include resolution effects on an event-by-event basis for the physics distributions, P_b, P_{bc}, and P_c, and to average over them in determining P_{dk} and P_{mis}.
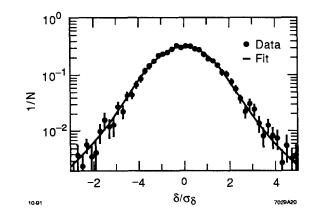
13

10-91   7029A20

Fig. 8. The impact parameter normalized by the calculated impact
parameter error for hadron tracks constrained to lie near the thrust
direction. The distribution is fit with the sum of two Gaussians.

The resolution function is $R(\delta, \sigma_\delta)$ is determined by measuring the impact pa-
rameters of hadronic tracks, and attempting to account for or minimize finite lifetime
effects that remain in this sample. Figure 8 shows the distribution of impact param-
eters divided by calculated errors observed by the MARK II experiment for a sample
of high-p_T hadrons closely aligned with the thrust axis, and is typical of the stud-
ies done by other experiments. The resolution function is approximately Gaussian.
All experiments find that the width of the core of the distribution is slightly under-
estimated, and that roughly 10% of tracks must be assigned to a second, broader
Gaussian to account for the tails. The uncertainties of these procedures contribute a
significant systematic error to the resultant B lifetime.

Maximum Likelihood Fit

The normalized impact parameter distribution, including resolution effects, can
be written

$$P'(\delta,\ \sigma_\delta,\ \tau_b) \ = f_b\, P'_b(\delta,\ \sigma_\delta,\ \tau_b) \ + \ f_{bc}\, P'_{bc}\,(\delta,\ \sigma_\delta,\ \tau_b,\ \tau_c)$$
$$+ \ f_c\, P'_c(\delta,\ \sigma_\delta,\ \tau_c) \ + \ f_{\mathrm{mis}}\, P_{\mathrm{mis}}(\delta) \ + \ f_{dk}\, P_{dk}(\delta) \quad . \tag{17}$$

The lifetime is derived from a maximum likelihood fit, where τ_b is varied to maximize

$$\ell n\, \mathcal{L} = \sum_i \ \ell n\ P'(\delta_i,\ \sigma_{\delta i},\ \tau_b) \quad , \tag{18}$$

and the sum extends over all lepton tracks of impact parameter δ_i and error $\sigma_{\delta i}$.

Figure 9 shows the results of all lepton impact parameter measurements made
to date. The field has advanced significantly since the MAC and MARK II measure-
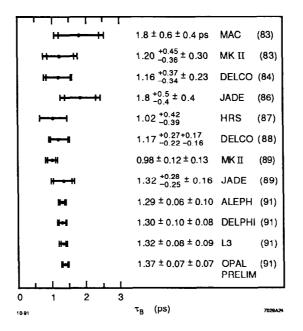ments of 1983. The measurements are in reasonable agreement, the worst discrepancy

14

Fig. 9. Lepton impact parameter measurements. The inner error bar gives the statistical error; the outer error bar the sum of the statistical and systematic errors in quadrature. The MARK II (89) and DELCO (88) measurements supersede the MARK II (83) and DELCO (84) measurements, respectively.

being the MARK II (89) measurement, which is 1.6 standard deviations below the current average, $\langle \tau_b \rangle = 1.29 \pm .03 \pm .07$ ps [30]. The LEP experiments, with good resolution and considerable statistical advantage, dominate the average. The measurement of the ALEPH Collaboration is representative, and is shown in Figure 10. To be precise, the B lifetime measured is an average overall B hadron species produced in e^+e^- annihilations, weighted by the product of their semileptonic branching ratios and their production cross sections. Strictly speaking, the PEP–PETRA average need not coincide perfectly with that from LEP, but most likely this difference is lost in the errors.

The procedure outlined above is clearly complex, and has some significant systematic errors associated with it.
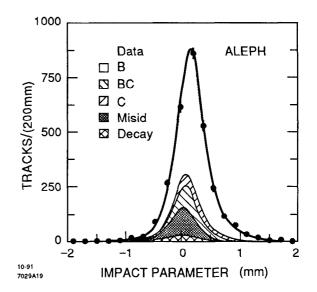

Fig. 10. The lepton impact parameter distribution measured by ALEPH (91), showing the overall fit to the data and the contributions from the various components of the signal.

15

At PEP–PETRA energies, the dominant systematic errors arise from uncertainties in B fragmentation, the fraction of high-p_T leptons due to B hadrons, and the resolution function. Overall, the errors range between 13 and 20%. At the Z^0, fragmentation effects are less important, but uncertainties in the B fraction, the resolution function, and the physics distributions used in the fit combine to give total systematic errors between 5 and 8%, rather evenly distributed among the sources.

Hadronic Impact Parameter Measurements

Most B decays are hadronic, as opposed to semileptonic, and most B decay products are hadronic. It follows that the bulk of the lifetime information content of the decays is carried in hadronic tracks. Measurements of the average hadron impact parameter [31] tap this additional information, and offer reduced statistical errors. The price for this improvement is considerably greater dependence on intricate and less well-known details of B production and decay, and ultimately a larger systematic error and less robust analysis. Even so, these analyses have been important confirmations that the B lifetime is, in fact, in the picosecond range. Besides, they measure an average B lifetime different in principle from that measured in the lepton impact parameter measurements. That is, they measure the average of the lifetimes of the various species of B hadrons, weighted by their respective production cross sections. In principle at least, differences in the average hadronic and average leptonic lifetimes let one infer that differences in the species lifetimes exist [32]. In practice, the accuracy of the measurements is not great enough to make significant conclusions.

The methods employed in measuring the average hadronic impact parameter $\langle \delta_h \rangle$ are, in general, similar to those discussed in detail above. However, event selection strategy is rather different from the lepton measurements. Two experiments (MAC and JADE (86)) do use a high-p_T lepton tag; but TASSO enriches the signal on the basis of a sphericity product, and the recent DELPHI measurement uses no enrichment at all. The other elements of the lepton impact parameter measurements are used: a projected impact parameter is measured with respect to the primary interaction point, and signed with reference to the jet direction. Several cuts are imposed on hadronic tracks, including a minimum momentum cut and tracking quality cuts. Event cuts are imposed to minimize contamination of the sample by 3-jet events, for which the B hadron direction is poorly determined. Very large impact parameters are excluded with a cut $|\delta| < 2 - 3$ mm. The MAC, TASSO (84), and DELPHI experiments measure the average hadron impact parameter. The JADE (86) and TASSO (89) experiments measure weighted hadronic impact parameters, where a weight factor is assigned event-by-event on the basis of the observed sphericity product, proportional to the probability that the event contains B hadrons. TASSO (89) additionally weights impact parameters inversely with the square of the impact parameter error.

The B lifetime is derived by comparing the mean hadronic impact parameter to values calculated from full Monte Carlo simulations for different B lifetimes. The principal systematic errors derive from the uncertainty in the sample composition, the bottom fragmentation function, and detector-related effects—especially impact parameter resolution. Uncertainty in the fragmentation variable $\langle x_B \rangle = 2\langle E_B \rangle / E_{CM}$
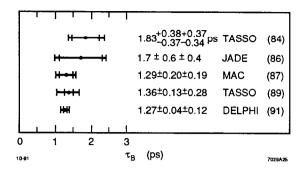
Fig. 11. Hadron impact parameter measurements. The inner error bar gives the statistical error; the outer error bar is the sum of the statistical and systematic errors in quadrature.

is especially significant, as it is correlated to the number of fragmentation tracks produced, and thus to $\langle \delta_h \rangle$. Experiments take care to reproduce in detail the average charged multiplicity of B decays and the average charged energy of the decay products, and in fact the myriad parameters needed to completely characterize the decays: charm particle production in B decays, charm particle lifetimes and decay multiplicities, and so on. MAC finds that uncertainties in fragmentation dominate the systematics with a 15% error; TASSO (89), after a thorough study of Monte Carlo parameters, is left with a 20% systematic error. DELPHI (91) claims a 10% systematic error, dominated by resolution and fragmentation effects.

The results of the experiments are shown in Fig. 11. The average B lifetime measured with hadron impact parameters is $1.32 \pm .04 \pm .12$ ps [30], dominated by DELPHI's result of $1.27 \pm .04 \pm .12$ ps, which is shown in Fig. 12. The result is clearly compatible with the lepton impact parameter measurements, and the 3% statistical precision illustrates the sensitivity of the method.

One window on the future of hadron impact parameter measurements is shown in Fig. 13, in which the MARK II Collaboration's measurement [33] of the sum of hadronic impact parameters in a jet, $\sum \delta_i$, measured at the SLC is plotted.
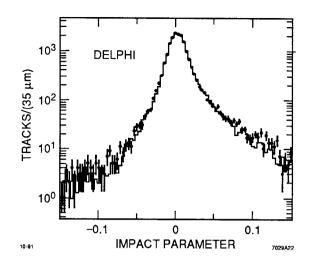

Fig. 12. Hadron impact parameter distribution measured by DELPHI (91) in an unenriched sample at the Z^0. The best fit to the distribution overlays the data.
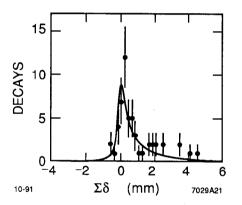

Fig. 13. The sum of impact parameters in B hadron jets at the Z^0, measured by the MARK II SLC Collaboration, and a best fit to the data. The exponential character of the distribution is apparent.

17

The MARK II SLC detector has a resolution in $\sum \delta_i$ well below the mean of the distribution that clearly reveals the exponential character of the B lifetime distribution. The sample is also unique, in that it was tagged by observing significant impact parameters ($\delta/\sigma_\delta > 3$) in the opposite jet. The result is weak statistically, but is compatible with other estimates of B lifetimes.

4. Other Average B Lifetime Measurements

In this section alternatives to the impact parameter methods for measuring b lifetimes are discussed. All of these "other" methods go beyond using information from a single track. Instead, an attempt is made to reconstruct the decay vertex of B hadrons and hence compute its laboratory decay length. We divide these vertexing methods into two categories that are distinguished from each other by either comparing a "B" vertex with the primary vertex (beam spot) or by comparing two "B" vertices to each other, therefore taking advantage of the fact B hadrons come in pairs.
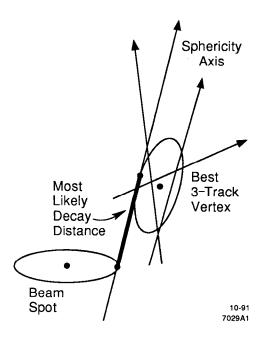

Fig. 14. Illustration of the vertex method. The best three-prong vertex in a jet is found, and the most likely decay distance from the beam spot is calculated, using the sphericity axis as an estimate of the flight direction of the B hadron.

There are two B lifetime measurements that compare a single reconstructed B-hadron vertex to the primary vertex (see Fig. 14). The first of these came from TASSO (89) [31]. This result was based on 31,000 hadronic events taken in 1986 with a "high-precision" vertex detector installed in the apparatus. Events were initially divided into two jets by grouping the tracks into the two hemispheres defined by the event sphericity axis. No effort was made to enrich the 1/11 mix of $b\bar{b}$ events. Inside each jet, an attempt was made to reconstruct a three-prong vertex from tracks that passed stringent track-quality cuts and have momenta > 0.6 GeV/c. The vertex fit was performed in the x-y plane, and was required to have a confidence level greater than 1%. The most probable three-prong vertex was selected in jets with more than one candidate. This procedure does not guarantee that the vertexed tracks are from the B, but Monte Carlo studies show significantly displaced vertices result from B decay. In excess of 13,000 decay distances were used in the final result, which gives $\tau_B = 1.30 \pm .10 \pm .28$ ps. The decay distance distribution along with the Monte Carlo prediction is shown in Fig. 15. The large systematic error reflects the heavy reliance on the Monte Carlo to calibrate this method.

The second result using a single B-hadron vertex is more recent and comes from the OPAL Collaboration at LEP [34]. A signal for J/ψ production is found using the
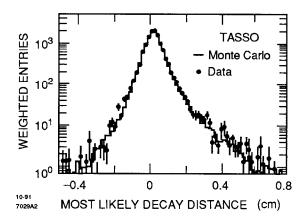
18

Fig. 15. Distribution of most likely decay distances. The points with error bars are the data. The solid line is a Monte Carlo distribution with $\tau_B = 1.30$ ps, which gives the best fit to the data.
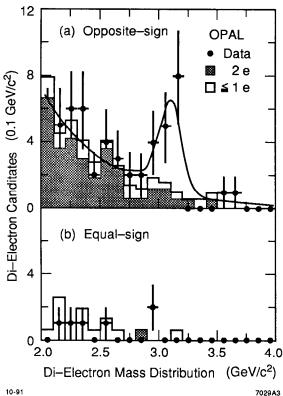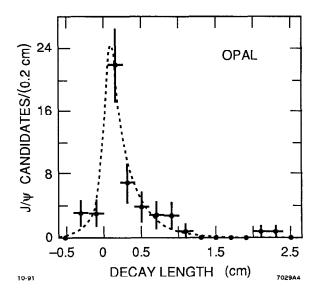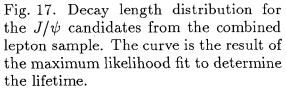
Fig. 16. The invariant mass distribution of e^+e^- candidate pairs is shown in (a) together with the result of a fit assuming signal and background shapes derived from the Monte Carlo. In (b) the invariant mass distribution for electron pairs with equal signs is shown. The Monte Carlo estimate for the background from two electrons is shown in black, the background including at least one misidentified electron is shown by the open histogram.

leptonic decay channels of this vector meson. A major background source for the J/ψ signal is the B-hadron cascade decays, in which a prompt lepton comes from both the b and subsequent c quark in the decay chain. However, this and other backgrounds are small compared to the signal which totals 45 events (see Fig. 16). The observed J/ψ's are attributed to B-hadron decays. Relevant to B lifetimes, these two prong leptonic J/ψ decays are ideal for vertexing. The decay length is calculated in the x-y plane from the positions of the decay vertex and the beam center (at LEP the beam size is 160 μm $\times$ 8μm), and extended to three dimensions using the polar angle of the nearest jet. The boost factor $(\gamma\beta)$ is estimated from the measured momentum of the J/ψ. The resulting distribution of decay lengths is shown in Fig. 17. A maximum likelihood fit has been used to determine the lifetime $\tau_B = 1.32 \, ^{+.31}_{-.25} \pm .15$ ps.

The second method used to measure generic B-hadron lifetimes has been applied by some PETRA experiments, and is referred to by names like "dipole length"

Fig. 17. Decay length distribution for the J/ψ candidates from the combined lepton sample. The curve is the result of the maximum likelihood fit to determine the lifetime.

Fig. 18. Illustration of the dipole moment. A vertex is found in each jet of an event, and the distance between them is calculated.

or "pseudo decay length." In this technique, a vertex is reconstructed in each jet in an event, and the distance between them is determined as a measure of the distance between the B and the $\bar{B}$ hadron vertices. The motivation is to eliminate the uncertainties in the location of the primary vertex and to increase the measured decay lengths relative to the experimental resolution. Of course, the penalty is that fewer events have enough quality racks to be included in the sample.

The TASSO (89) Collaboration has employed such a technique [31], which we now describe. Events are divided into two jets using the sphericity axis, which is taken to be the direction of the B and $\bar{B}$ hadrons, assumed to be going in opposite directions. The projection of the sphericity axis in the x-y plane is translated to minimize the variance of the crossing points of the tracks and is hence called the "event" axis, shown in Fig. 18. All the tracks in a jet are then used to form a vertex point along this event axis. The tracks are weighted by rapidity and $\sin^2 \alpha$ where α is the crossing angle between the track and the event axis. It is claimed that this weighting reduces the sensitivity to variations in heavy quark fragmentation as well as enhancing first rank decay particles from the B hadrons. The distance between the reconstructed vertices in each jet is called the dipole moment, and can be negative. The distribution of dipole moments is shown in Fig. 19.

The statistics, although high (greater than 19,000 measured dipole moments), contain only 9% $b\bar{b}$ events (i.e., no different from the generic 1/11). As such the "signal" is quite dilute, and the Monte Carlo must be relied on to accurately predict this distribution—not only for $b\bar{b}$, but for $c\bar{c}$, as well as the light quarks. The final result is $\tau_B = 1.47 \pm .14 \pm .30$ ps.
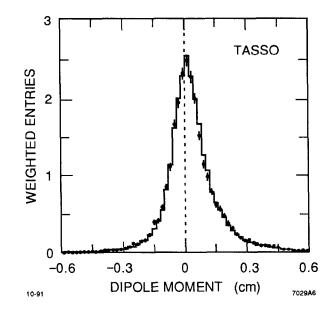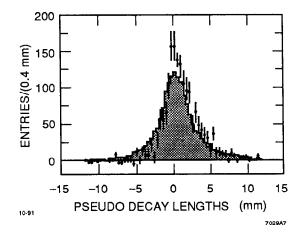
Fig. 19. Distribution of dipole moments. The points with error bars are the data, and the solid line is a Monte Carlo distribution with $\tau_B = 1.50$ ps. A bin-by-bin comparison of the two distributions gives a total χ^2 of 70.6 for 60 bins.

The JADE (90) Collaboration has performed a similar analysis [24]. Events are divided into two jets along the sphericity axis. Each jet is "verticized" in the x-y plane and forced to lie on the sphericity axis. Differing from the TASSO approach, the formation of the vertices is done without special weights for each track, but event-by-event weights are used to enhance the $b\bar{b}$ signal. This event weight is formed by taking the product of the boosted sphericities for each jet ($S_1 \times S_2$), as discussed in the last section. As with the "dipole length" method, heavy reliance on the Monte Carlo for calibrating the method is required, resulting in an appreciable systematic error. There is also substantial background (see Fig. 20). They find $\tau_B = 1.46 \pm .22 \pm .34$ ps.

Figure 21 shows the results of these average B-hadron lifetime measurements. As the figure indicates, they are consistent with the lifetime determined from lepton impact parameters.

5. Specific B-Hadron Lifetime Measurements

The physics interest in comparing the lifetime of various types of B hadrons is to probe our understanding of the mechanism of the decay, and to this end several efforts have been made to measure B^0 and B^+ meson lifetimes. All of these measurements fall into the reconstructed vertex category, rather than the impact parameter method. This naturally follows since to separate B^0 and B^+ mesons, many of the decay tracks must be identified. Once this is done, they can be used to reconstruct the decay vertex.
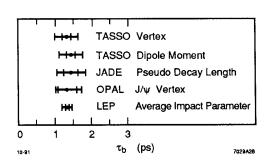
Fig. 20. Pseudo-Decay-Length distribution of the signal sample (shown as data points) and a background sample (shown as shaded histogram).

Fig. 21. Non-Impact Parameter B-hadron lifetime measurements. The LEP Average Impact Parameter result is included for comparison.

Indirect Methods for Measuring Lifetime Ratios

There is an alternative to directly measuring B meson lifetime ratios, and that is to infer them from the semileptonic branching ratios. This has been done for both the CLEO and the ARGUS data [35]. In the approximation that the V_{ub} contribution is negligible, it follows easily that

$$\frac{\tau_{B^+}}{\tau_{B^0}} = \frac{\Gamma_{B^0-\mathrm{sl}}}{Br_{B^0-\mathrm{sl}}} \cdot \frac{Br_{B^+-\mathrm{sl}}}{\Gamma_{B^+-\mathrm{sl}}} = \frac{Br_{B^+-\mathrm{sl}}}{Br_{B^0-\mathrm{sl}}} \equiv \frac{b_+}{b_0} \quad , \tag{19}$$

under the assumption that the semileptonic decay rates for B^0 and B^+ are equal. In defense of this assumption, it may be observed that in the D meson system, even though the lifetimes of D^+ and D^0 are different, their semileptonic widths are equal. This assumption is also what is predicted to be the case in the QCD corrected spectator model for B decays.

To measure the B^+ and B^0 semileptonic branching ratios, b_+ and b_0, the most obvious approach is to reconstruct D's and D^*'s in association with the prompt leptons: $B^+ \to \bar{D}^0 \ell^+ \nu$, $\bar{D}^{*0} \ell^+ \nu$ and $B^0 \to D^- \ell^+ \nu$, $D^{*-} \ell^+ \nu$. Under the assumption that the fraction of $D\ell\nu$ and $D^*\ell\nu$ final states are the same for B^0 and B^+, one may use these branching ratios in Eq. 19 . There is, however, one more unknown: the ratio of the rates for $\Upsilon_{4s} \to B^0 \bar{B}^0$ to $\Upsilon_{4s} \to B^+ B^-$, (f_{00}/f_{+-}). The answer is quoted including this factor [35]:

$$\frac{\tau_{B^+}}{\tau_{B^0}} = \left(\frac{f_{00}}{f_{+-}}\right) \begin{cases} (\,.89 \pm .19 \pm .13) & \text{CLEO} \\ (1.00 \pm .23 \pm .14) & \text{ARGUS} \end{cases} . \tag{20}$$

22

An alternative to reconstructing charm final states is to measure the number of high-p_T single-lepton events and high-p_T dilepton events [36]. The expected numbers for these can be written:

$$N_\ell = 2 \left(f_{00}\, b_0 + f_{+-}\, b_+ \right) N_{B\bar{B}} \quad,$$

$$N_{\ell\ell} = \left(f_{00}\, b_0^2 + f_{+-}\, b_+^2 \right) N_{B\bar{B}} \quad. \tag{20}$$

where $N_{B\bar{B}}$ is the number of $B\bar{B}$ pairs in the event sample. Since $N_{\ell\ell}$ is quadratic in b_0 and b_+, one may solve for the ratio b_+/b_0. It turns out that this method is quite insensitive to the ratio of f_{00}/f_{+-} and also is independent of the charm ratio assumption. The problem is that Eq. 21 is symmetric in b_0 and b_+, and for physical values of $(N_\ell^2/N_{\ell\ell})$, the ratio (b_+/b_0) will have two solutions. Near the expected value $(\tau_{B+} \simeq \tau_{B^0})$, $(N_\ell^2/N_{\ell\ell})$ is not a very sensitive indicator. The result is [37] $\tau_{B+}/\tau_{B^0} = b_+/b_0 = 1.0\,^{+.49}_{-.32}$.

Direct Measurements of Specific B-Hadron Lifetimes

The MARK II Collaboration published the first measurement of the lifetime of a specific B meson using their PEP data [38]. Starting from an enriched B sample, events tagged with a high-p_T lepton, they further require the partial reconstruction of a D^*, looking for the decay chain,

$$
\begin{aligned}
B^\circ &\to D^{*-} X \ell^+ \nu \\
D^{*-} &\to \pi^- \bar{D}^0 \\
\bar{D}^0 &\to K^+ \pi^- X \ .
\end{aligned}
\tag{22}
$$

The (bachelor) pion from the D^{*-} decay is required to lie in the same hemisphere as the tagging lepton, and have momentum $0.1 < p < 1.0$ GeV/c. The $\bar{D}^0$ was partially reconstructed by combining the remaining charged and neutral tracks that had a component of momentum along the thrust axis greater than .5 GeV/c and 1.0 GeV/c, respectively. All tracks were assigned the pion mass, except for the highest momentum track with charge opposite the D^* decay pion; it was chosen to be the kaon. The mass difference (Δm) between this track combination with and without the bachelor pion is given in Fig. 22, and shows the famous D^* signal (albeit broadened due to the partial reconstruction of the $\bar{D}^0$).

The authors then reason, based on simple physical assumptions and detailed Monte Carlo studies that approximately $83 \pm 8\%$ of this signal is in fact due to $\bar{B}^0$ decay. The vertex of the $\bar{B}^0$ is calculated by first determining the $\bar{D}^0$ vertex, and then intersecting the $\bar{D}^0$ trajectory with that of the high-p_T lepton. The bachelor pion is not used in the vertex due to its large multiple scattering. The vertexing calculation is made in the x-y plane, and the polar angle is taken to be that of the $D^*\ell$ pair. This pair is also used to evaluate the boost factor for the B^0.
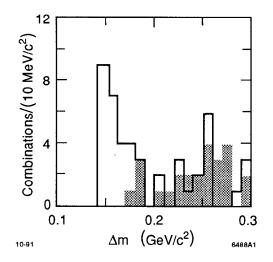
Fig. 22. The Δm distribution for all $\bar{D}^0$-candidate–bachelor–pion combinations for which the bachelor pion has charge opposite that of the high-p_T lepton in the same thrust hemisphere (solid line), and for which the bachelor pion has the same charge as the lepton (hatched area).

The resulting 15 events are shown in Fig. 23, and are used as input to a maximum likelihood fit with the result $\tau_{B^0} = 1.20^{+.52\ +.16}_{-.36\ -.14}$ ps. The authors have checked their work by producing in Monte Carlo B^0 meson lifetimes ranging from .6 to 1.6 ps, and found that the analyzed lifetimes agree well with the input.
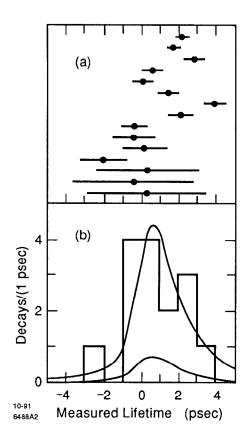
Fig. 23. The (a) fifteen B^0-lifetime measurements and their errors, and (b) a histogram of the measurements, with the fitted signal and background curve (solid), and the background curve (dashed) overlaid.

A recent measurement following along similar lines comes from the ALEPH Collaboration at LEP [39]. In their prompt lepton sample, a D^0 as well as D^{*+} signal is found. In both cases a $D^0 \to K^-\pi^+$ is reconstructed.

For the $D^{*+} \to D^0\pi^+$ signal all tracks inside a 45° cone around the prompt lepton track are considered. Tracks with the same charge as the lepton are tried as kaons, while oppositely charged tracks are assigned to be pions. To each D^0 candidate a third track is added to form the D^{*+}. A high-quality D^* signal with estimated background $\sim 11\%$ (see Fig. 24(a)) is isolated using the mass difference $M_{D^{*+}} - M_{D^0}$, the D^* momentum, the angle between the kaon and the D^0 and, finally, the mass of the D^0.

To find a D^0 (as opposed to D^{*+}) signal is more difficult and the dE/dx information from the main tracking chamber [40] is used to select kaon candidate tracks.
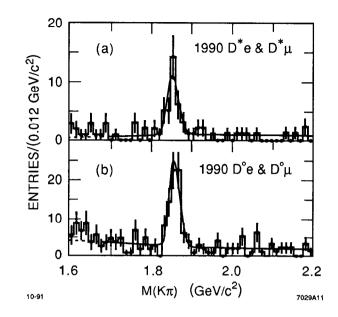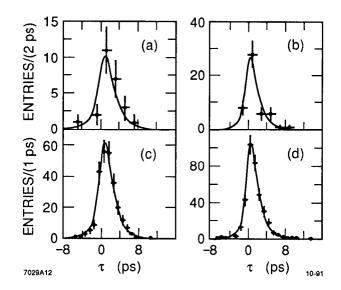
24

Fig. 24. Results of fits to the $K\pi$ mass distributions for (a) $D^{*+}\ell^-$ correlations, and (b) $D^0\ell^-$ correlations.

A higher momentum cut is also placed on the D^0 momentum. The result is a D^0 signal with an estimated background of 17.5% [see Fig. 24(b)].

The vertexing is similar to what was done in the MARK II analysis: a D^0 "track" is formed and "verticized" with the prompt lepton. The primary vertex is taken to be the beam centroid. The D meson and prompt lepton are combined to form a candidate B meson. The polar angle of this combination is used to compute the three-dimensional decay length from the projected decay length. The boost factor is also taken from this pair, then corrected up by 19% to account for the missing neutrino. The resulting proper decay lengths are shown in Fig. 25, along with the Monte Carlo signals. Fits give lifetimes $\tau_{D^*\ell} = 1.42\pm^{.54}_{.41}$ ps and $\tau_{D^0\ell} = 1.35\pm^{.36}_{.29}$ ps.

Estimates are then made of the relative amount of B^+ and B^0 (as well as background) in these two samples. As in the MARK II analysis, $D^{*+}\ell^-$ is found to be dominated by B^0 decays, and B^0/B^+ fractions are introduced into the fit with the results $\tau_+ = 1.35\,^{+.42}_{-.46}$ ps and $\tau_0 = 1.42\,^{+.52}_{-.48}$ ps. They find for the ratio $\tau_+/\tau_0 = .96\,^{+.69}_{-.49}$. The ALEPH and MARK II results agree quite well, although with large errors. Also these results are consistent with the lifetime ratios derived by CLEO and ARGUS.

The last experiment we review, now reporting on b^+ and b^0 lifetimes, is the fixed target experiment at Fermilab, E653 [41]. (In fact, this is the first fixed target experiment to report on direct B-hadron observations since the solitary event observed in the CERN experiment, WA75 [42] in 1985.) Note that this experiment does not specify whether the observed hadrons are baryons or mesons (hence the lower case 'b'). A wide range of technologies is employed, as shown in Fig. 26. The heart of the experiment is a 1.5-cm-thick emulsion target and several "decay analyzers" (essentially

Fig. 25. The proper time distributions for the $D^{*+}\ell^-$ and $D^0\ell^-$ samples (a,b). The dashed lines are the fit results. Also shown (c,d) are fits to the Monte Carlo signal events.

thin emulsion films placed 1.2 and 2.2 cm downstream of the target). The emulsions are followed by a silicon microstrip detector, an analyzing dipole magnet, and 55 planes of drift chamber complete the tracking. This is followed by a liquid argon calorimeter, and then an iron drift-chamber muon analyzer. The incident beam was a 600 GeV/c π^- beam , and the full exposure produces about 2.5×10^8 recorded interactions.
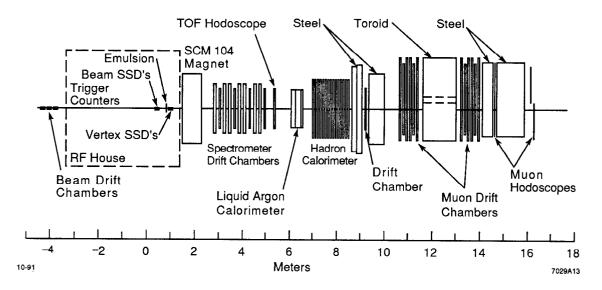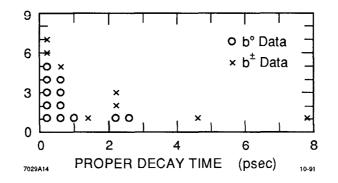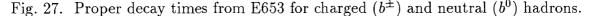

Fig. 26. Layout of FERMILAB Experiment E653.

Fig. 27. Proper decay times from E653 for charged ($b^{\pm}$) and neutral (b^0) hadrons.

The data sample selected for scanning required a muon with $p_\mu > 8$ GeV/c. The muon was also required to have a transverse momentum with respect to the beam of at least 1.5 GeV/c. Primary vertices are found in these events with high efficiency— claimed to be $\sim 99\%$! "Interesting" events are selected when none of the tracks from the primary vertex match with the muon track (within ~ 2 mrad). The event is then carefully scanned, first following tracks downstream through the emulsion to locate all associated charged decays. A detailed program, matching the spectrometer tracks to the emulsion, then follows. A frequently occurring background comes from e^+e^- pairs due to photon conversions, but these along with nuclear breakup tracks are easily identified and rejected.

The first scan resulted in 351 events, of which the major fraction was identified to be from charm events (165 of the total). Secondary interactions and $K^{\pm} \to \mu^{\pm}\nu$ decays accounted for another 168 events, leaving 16. Of these, half had muons where the origin of the muon was unclear, but the other half are identified as $b\bar{b}$ candidates.

A second scan now in progress lowers the p_T requirement on the muon to .8 GeV/c, and in addition requires the presence of another hadron track with a $p_T > 1$ GeV/c. To date this scan has revealed two more $b\bar{b}$ events. In the first scan all the muons are found to come from the B-hadron decay, while in the second scan the two events found so far have the muons originating at the tertiary, charm vertices.

The minimum mass [43], Feynman x, and transverse momentum of the 20 partially reconstructed B hadrons agree well with the expectations of the production model. This adds credibility to the assertion that these are indeed $b\bar{b}$ events. The Lorentz boost γ is estimated from the visible mass and energy, with a typical error of $\pm 25\%$.

The proper decay times for these 20 B-hadronic decays are shown in Fig. 27. A maximum likelihood fit gives the results $\tau_{\mathrm{ALL}} = 1.65^{+.6}_{-.4}$ ps (20 decays), $\tau_{b^0} = .95^{+.5}_{-.3}$ ps (12 decays), and $\tau_{b^{\pm}} = 2.5^{+2.0}_{-.8}$ ps (8 decays). The E653 group also state that the probability that $\tau_{b^0} = \tau_{b^{\pm}}$ is about 5%. The statistics are quite low, so this can't, as yet, be viewed to be in conflict with the result coming from e^+e^- annihilations.

The measurements of lifetime ratios and individual B hadrons are summarized in Figs. 28 and 29, respectively. Nothing extraordinary has as yet turned up, and indeed these early measurements seem to be confirming the conjecture that B hadrons will all have very similar lifetimes.
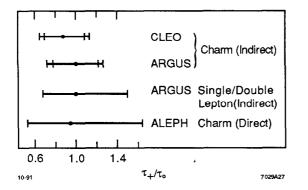
Fig. 28. Ratio of the charged to neutral B-hadron lifetime. Notice that only the ALEPH measurement is the ratio of measured lifetimes; the others are inferred from branching ratios and lepton counting.
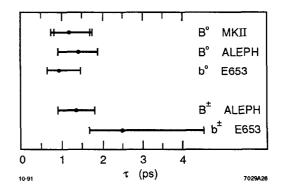

Fig. 29. Lifetimes of specific B hadrons.

6.   Outlook and Conclusions

The measurement of B-hadron lifetimes has made a significant contribution to our overall understanding of quark generation mixing. The early measurements of long B lifetimes surprised many of us, and were the first to fix the magnitude of the CKM parameters beyond the two-generation quark model. The first measurements analyzed the average impact parameters of prompt leptons. The apparatus resolution for measuring these lifetimes was at best comparable to the lifetime itself, and the effects were subtle. Extracting the B lifetime required in-depth understanding of the experimental resolution, as well as knowledge of B-hadron production and decay.

A decade of refinement has now passed and in the latest round of measurements from LEP, B lifetimes with errors less than 10% have been published. Improvements in tracking have slowly nibbled away at the resolution issues. Together with measurements of B semileptonic branching ratios and the theory of B semileptonic decays, the present B lifetime measurements provide the most accurate means presently available for extracting the CKM matrix element V_{cb}. In fact, uncertainties in the extraction of V_{cb} are dominated by the theoretical corrections, rather than the statistical or systematic experimental errors in the lifetime.

The fact that the B lifetime is long is additional evidence that the top quark exists. Without substantial mixing to top, the greatly suppressed decay rate of the b is unexplained and would constitute a violation of weak universality.

Improvements in lifetime measurements can be expected from the new generation of high-resolution tracking devices . The reconstruction and vertexing of specific B hadrons will pave the way for detailed studies of the properties of B_u, B_d, B_s, and B_{baryons}. With the advent of high-statistics data sets, we look forward to precise measurements of the individual B hadron lifetimes.

28

The "sleeping giants" in the field are experiments at the hadron accelerators. We have now seen the beginnings of fixed target results, and soon expect collider experiments such as CDF at Fermilab to produce lifetime measurements. The unquestioned advantage of the hadron colliders is rate. The disadvantages are event complexity and high backgrounds. Both of these disadvantages are being overcome, however, and already impressive, fully reconstructed B meson signals have been shown by CDF.

We close by noting that B-lifetime measurements and B-hadron tagging will be of vital interest in the future, extending into the domains of neutral B meson mixing, studies of CP violation, and searches for the top quark.

Acknowledgments

References

1. MAC Colaboration, E. Fernandez *et al., Phys. Rev. Lett.* **51** (1983) 1022.
2. MARK II Colaboration, N. S. Lockyer *et al., Phys. Rev. Lett.* **51** (1983) 1316.
3. V. Barger, W. F. Long, and S. Pakvasa, *J. Phys.* **G5** (1979) L147.
4. H. Harari, SLAC–PUB–2234 (1978).
5. D. Cutts *et al., Phys. Rev. Lett.* **41** (1978) 363; R. Vidal *et al., Phys. Lett.* **B77** (1978) 344.
6. JADE Colaboration, W. Bartel *et al., Z. Phys.* **C6** (1980) 295.
7. JADE Colaboration, W. Bartel *et al., Phys. Lett.* **B114** (1982) 71.
8. CLEO Collaboration, A. Chen *et al., Phys. Rev. Lett.* **52** (1984) 1084; CUSB Collaboration, C. Klopfenstein *et al., Phys. Lett.* **B130** (1983) 444.
9. P. Ginsparg and M. Wise, *et al., Phys. Lett.* **127B** (1983) 265; L. L. Chau in *Proc. Physics in Collision 3*, (Como, Italy) 1983.
10. E. Paschos, B. Stech and U. Türke, *Phys. Lett.* **B128** (1983) 240;
11. P. Ginsparg, S. Glashow, M. Wise, *et al., Phys. Rev. Lett.* **501** (1983) 1415.
12. We use units such that $\hbar = c = 1$.
13. CLEO Collaboration, R. Fulton *et al., Phys. Rev. Lett.* **64** (1990) 16. ARGUS Collaboration, H. Albrecht *et al., Phys. Lett.* **B255** (1991) 297.
14. G. Altarelli *et al., Nucl. Phys.* **B208** (1982) 365.
15. CLEO Collaboration, E. H. Thorndike, *Proc. 1985 Int. Sym. on Lepton and Photon Interactions at High Energies,* eds. M. Konumu and K. Takahashi (Kyoto, 1986) p. 406. ARGUS Collaboration, H. Albrecht *et al., Phys. Lett.* **B249** (1990) 359.
16. For example, see L3 Collaboration, B. Adeva *et al.,* preprint L3–32, July 1991 (submitted to *Phys. Lett.*). Notice that these authors have included the QCD correction, as well as the phase space factor, in the definition of $F(\epsilon)$. Also see Chaps. 9 and 3, this volume.

17. C. S. Kim and A. D. Martin, *Phys. Lett.* **B225** (1989) 186.
    N. Cabibbo and L. Maiani, *Phys. Lett.* **B19** (1978) 109.
    M. Suzuki, *Nucl. Phys.* **B145** (1978) 420.
    A. Ali and E. Picturinen, *Nucl. Phys.* **B154** (1979) 519.

18. This value for α_s results from an extrapolation from LEP energies to m_b.
    α_s is believed to be well determined at LEP energies. For example:
    ALEPH Collaboration, D. Decamp *et al.*, *Phys. Lett.* **B257** (1991) 479,
    DELPHI Collaboration, P. Abreu *et al.*, *Phys. Lett.* **B252**, (1990) 149,
    OPAL Collaboration, M. Z. Akrawy *et al.*, *Phys. Lett.* **B252** (1990) 159,
    L3 Collaboration, B. Adeva *et al.*, *Phys. Lett.* **B248** (1990) 464 and **B257** (1990) 469.

19. M. Wirbel, B. Stech, and M. Bauer, *Z. Phys.* **C29** (1985) 637.

20. B. Grinstein, N. Isgur, M. B. Wise, *Phys. Rev. Lett.* **56** (1986) 298.
    B. Grinstein, N. Isgur, D. Scora, M. B. Wise, *Phys. Rev.* **D39** (1989) 799.

21. M. K. Gaillard and B. W. Lee, *Phys. Rev. Lett.* **33** (1974) 108.
    G. Altarelli and L. Maiani, *Phys. Lett.* **B52** (1974) 351.
    Also see F. Gilman, *Proc. 14th SLAC Summer Institute on Particle Physics,*
    ed. E. Brennan, p. 191, for a comprehensive review of hadronic B decays.

22. T. Sjöstrand, Comput. Phys. Commun. **28** (1983) 29.

23. See, for example, OPAL Collaboration M. Z. Akraiuy *et al.*, *Phys. Lett.* **B263** (1991) 311, and references cited therein.

24. MAC (83), E. Fernandez *et al.*, *Phys. Rev. Lett.* **51** (1983) 1022;
    MARK II (83), N. S. Lockyer *et al.*, *Phys. Rev. Lett.* **51** (1983) 1316;
    DELCO (84), D. E. Klem *et al.*, *Phys. Rev. Lett.* **53** (1984) 1873;
    JADE (86), W. Bartel *et al.*, *Z. Phys.* **C31** (1986) 349;
    HRS (86), J.-M. Brom *et al.*, *Phys. Lett.* **195** (1987) 301;
    DELCO (88), D. E. Klem *et al.*, *Phys. Rev.* **D37** (1988) 41;
    MARK II (89), R. A. Ong *et al.*, *Phys. Rev. Lett.* **62** (1989) 1236;
    JADE (90), J. Hagemann *et al., Z. Phys.* **C48** (1990) 401.

25. ALEPH (91), D. Decamp *et al.*, *Phys. Lett.* **B257** (1991) 492;
    DELPHI (91), P. Abreu *et al.*, CERN–PPE/91-131 (1991),
    submitted to *Z. Phys. C*;
    L3 (91), B. Adeva *et al.*, L3 Preprint 32 (1991);
    OPAL (91), Preliminary result reported by Dean Karlen at DPF '91,
    Vancouver, OPAL Conf. Report CR028.

26. MARK II Collaboration, R. Jacobsen *et al.*, SLAC–PUB–5603 (1991),
    submitted to Phys. Rev. Lett.

27. W. T. Ford in *Proc. Third MARK II Workshop on SLC Physics,* SLAC Report 315 (1987).

28. R. A. Ong, Ph.D. Thesis, SLAC Report 320 (1987). These values are appropriate at PEP energies.

29. S. Petrera and G. Romano, *Nucl. Inst. Meth.* **174** (1980) 61.

30. The individual results have been weighted by the inverse square of the total error in computing the average. The systematic error has been set equal to the smallest of the systematic errors reported.

31. TASSO (84), M. Althoff *et al.*, *Phys. Lett.* **B149** (1984) 524;
JADE (86), W. Bartel *et al.*, *Z. Phys.* **C31** (1986) 349;
MAC (87), W. W. Ash *et al.*, *Phys. Rev. Lett.* **58** (1987) 640;
TASSO (89), W. Braunschweig et al., *Z. Phys.* **C44** (1989) 1;
DELPHI (91), P. Abreu *et al.*, CERN–PPE/91–131 (1991),
submitted to *Z. Phys. C.*

32. J. Jaros in *Proc. Physics in Collision 4* (Santa Cruz) 1984.

33. MARK II Collaboration, D. Fujino in *Proc. Division of Particles and Fields Conf.* (Vancouver, BC) 1991.

34. OPAL Collaboration, G. Alexander *et al.*, CERN–PPE/91–92 (1991), submitted to Phys. Lett.

35. CLEO Collaboration, R. Fulton *et al.*, *Phys. Rev.* **D43** (1991) 651;
ARGUS Collaboration, H. Albrecht *et al.*, *Phys. Lett.* **B232** (1989) 554.

36. CLEO Collaboration, M. Artuso *et al.*, *Phys. Rev. Lett.* **58** (1987) 183.

37. ARGUS Collaboration, H. Albrecht *et al.*, DESY preprint DESY–91–056 (1991).

38. MARK II Collaboration, S. R. Wagner *et al.*, *Phys. Rev. Lett.* **64** (1990) 1095.

39. ALEPH Collaboration, preliminary results presented at the *Int. Symp. on Lepton and Photon Interactions at High Energy* (Geneva, Switzerland) August 1991.

40. W. B. Atwood *et al.*, *Nucl. Instrum. Methods* **A306** (1991) 446.

41. "Beauty Pairs and Charm Semileptonic Decays from Fermilab E653," presented by Noel R. Stanton at the *3rd Topical Seminar on Heavy Flavors* (San Miniato, Italy) June 1991.

42. J. P. Albanese *et al.*, *Phys. Lett.* **B158** (1985) 186.

43. $M_{\mathrm{MIN}} = p_T + \sqrt{m_{\mathrm{VIS}}^2 + p_T^2}$. See K. Kodama *et al.*, *Phys. Rev. Lett.* **66** (1991) 1819.